High-Performance, Stable Organic Field-Effect Transistors Based on *trans*-1,2-(Dithieno[2,3-*b*:3′,2′-*d*]thiophene)ethene

Lei Zhang, Lin Tan, Zhaohui Wang,* Wenping Hu,* and Daoben Zhu

Beijing National Laboratory for Molecular Science, Key Laboratory of Organic Solid, Institute of Chemistry, Chinese Academy of Sciences, Beijing 100190, P.R. China

Received February 9, 2009. Revised Manuscript Received March 26, 2009

We present here the synthesis, characterization, and transistor performance of three semiconductor materials based on *trans*-1,2-(dithieno[2,3-*b*:3′,2′-*d*]thiophene)ethene derivatives. Although the incorporation of aromatic, alkyl substituents in both ends of *trans*-1,2-(dithieno[2,3-*b*:3′,2′-*d*]thiophene)ethene have a negligible effect on the conjugation length and the energy gap, the subtle chemical modification leads to great variations in film microstructures, electronic properties, and packing arrangements. The appropriate substituents are capable of providing efficient molecular packing arrangements for high carrier mobility. The phenyl-substituted derivative, compound **3**, demonstrates a remarkably high thin film FET performance, with mobility up to 2.0 $cm^2\ V^{-1}\ s^{-1}$ and on/off ratio up to 10^8. In addition, the devices show good environmental stability, even after storage in air for 7 months.

Introduction

The synthesis of high performance organic semiconductors has been spurred up in recent years because of their applications for flexible, low-cost, and large-area electronic components.[1] Significant progress has been achieved by the development of new materials such as π-conjugated polymers, heteroacenes, and their derivatives.[2] Among these materials, oligo- and polythiophenes are important representative systems because of their synthetic availability, widespread possibility, and tunable electronic properties.[3]

In contrast to polythiophenes, fused-ring thienoacenes have more rigid structures, better conjugation, and larger band gaps. Furthermore, the extended π system in a molecule is expected to provide more efficient π orbital overlap and lead to high charge carrier mobility.[4] Particularly, in sulfur-rich annelated oligomers, the molecular packing is characterized by the cooperation of multiple S···S interactions and $\pi-\pi$ interactions, which may increase the effective dimensionality of the electronic structure, leading to enhanced transport properties. The relevant examples are sulfur decorated oligoacenes, in which S···S interactions provide an alternative charge transport pathway other than $\pi-\pi$ interactions.[5] Unfortunately, there are only a few examples using fused thiophene systems for organic field-effect transistors because of the limited synthetic approaches and the poor solubility of these compounds. So far, only pentathienoacene, the α-linked dimer of dithieno[3,2-*b*:2′,3′-*d*]thiophene and its alkylated derivatives, have been succeeded in being preparing as the active layers in organic thin film transistors. However, the mobility of these compounds is not yet satisfied (0.05 $cm^2\ V^{-1}\ s^{-1}$ for the dimer of dithieno[3,2-*b*:2′,3′-*d*]thiophene and 0.045 $cm^2\ V^{-1}\ s^{-1}$ for pentathienoacene).[4c,6] Recently, we reported a novel high performance organic semiconductor based on β-trithiophenes units, namely, *trans*-1, 2-(dithieno[2,3-*b*:3′,2′-*d*]thiophene)ethene, which exhibits a unique molecular packing motif and good device performance.[7] To tune the

* To whom correspondence should be addressed. E-mail: wangzhaohui@iccas.ac.cn (Z.W.),huwp@iccas.ac.cn (W.H.).

(1) (a) Halls, J. J. M.; Walsh, C. A.; Greenham, N. C.; Marsegia, E. A.; Friend, R. H.; Moratti, S. C.; Holms, A. B. *Nature (London)* **1995**, *376*, 498–500. (b) Garnier, F.; Hajlaoui, R.; Yassar, A.; Srivastava, P. *Science* **1994**, *265*, 1684–1686. (c) Greenham, N. C.; Moratti, S. C.; Dradley, D. D. C.; Friend, R. H.; Holms, A. B. *Nature (London)* **1993**, *365*, 628–630. (d) Drury, C. J.; Mutsaers, C. M. J.; Matters, M.; De Leeuw, D. M. *Appl. Phys. Lett.* **1998**, *73*, 108–110.

(2) (a) Murphy, A. R.; Fréchet, J. M. J. *Chem. Rev.* **2007**, *107*, 1066–1096. (b) Zaumseil, J.; Sirringhaus, H. *Chem. Rev.* **2007**, *107*, 1296–1323. (c) Reese, C.; Bao, Z. *Mater. Today* **2007**, *10*, 20–27. (d) Facchetti, A. *Mater. Today* **2007**, *10*, 28–37. (e) Salleo, A. *Mater. Today* **2007**, *10*, 38–45.

(3) (a) Sakai, N.; Prasad, G. K.; Ebina, Y.; Takada, K.; Sasaki, T. *Chem. Mater.* **2006**, *18*, 3596–3598. (b) Ong, B. O.; Wu, Y.; Liu, P.; Gardner, S. *Adv. Mater.* **2005**, *128*, 4911–4916. (c) Ling, M. M.; Bao, Z. *Chem. Mater.* **2004**, *16*, 4824–4840. (d) Heeney, M.; Bailey, C.; Genevicius, K.; Shkunov, M.; Sparrowe, D.; Tierney, S.; McCulloch, I. *J. Am. Chem. Soc.* **2005**, *127*, 1078–1079. (e) McCulloch, I.; Heeney, M.; Bailey, C.; Genevicus, K.; Macdonald, I.; Shkunov, M.; Sparrowe, D.; Tierney, S.; Wagner, R.; Zhang, W.; Chabinyc, M. L.; Kline, R. J.; Mcgehee, M. D.; Toney, M. F. *Nat. Mater.* **2006**, *16*, 328–333.

(4) (a) Zhang, X.; Côté, A. P.; Matzger, A. *J. Am. Chem. Soc.* **2005**, *127*, 10502–10503. (b) Osuna, R. M.; Zhang, X.; Matzger, A. J.; Hernandez, V.; Navarrete, J. T. L. *J. Phys. Chem. A* **2006**, *110*, 5058–5065. (c) Xiao, K.; Liu, Y.; Qi, T.; Zhang, W.; Wang, F.; Gao, J.; Qiu, W.; Ma, Y.; Cui, G.; Chen, S.; Zhan, X.; Yu, G.; Qin, J.; Hu, W.; Zhu, D. *J. Am. Chem. Soc.* **2005**, *127*, 13281–13286. (d) He, M.; Zhang, F. *J. Org. Chem.* **2007**, *72*, 442–451.

(5) (a) Sun, Y.; Tan, L.; Jiang, S.; Qian, H.; Wang, Z.; Yan, D.; Di, C.; Wang, Y.; Wu, W.; Yu, G.; Yan, S.; Wang, C.; Hu, W.; Liu, Y.; Zhu, D. *J. Am. Chem. Soc.* **2007**, *129*, 1882–1883. (b) Briseno, A. J.; Miao, Q.; Ling, M.; Reese, C.; Meng, H.; Bao, Z.; Wudl, F. *J. Am. Chem. Soc.* **2006**, *128*, 15576–15577. (c) Bromley, S. T.; Mas-Torrent, M.; Hadley, P.; Rovira, C. *J. Am. Chem. Soc.* **2004**, *126*, 6544–6545. (d) Xue, J.; Forrest, S. R. *Appl. Phys. Lett.* **2001**, *79*, 3714–3716.

(6) (a) Li, X.-C.; Sirringhaus, H.; Garnier, F.; Holmes, A. B.; Moratti, S. C.; Feeder, N.; Clegg, W.; Teat, S. J.; Friend, R. H. *J. Am. Chem. Soc.* **1998**, *120*, 2206–2207. (b) Sirringhaus, H.; Friend, R. H.; Li, X. C.; Moratti, S. C.; Holms, A. B.; Feeder, N. *Appl. Phys. Lett.* **1997**, *71*, 3871–3873. (c) Morrison, J. J.; Murray, M. M.; Li, X. C.; Holms, A. B.; Morratti, S. C.; Friend, R. H.; Sirringhaus, H. *Synth. Met.* **1999**, *102*, 987–988.

(7) Tan, L.; Zhang, L.; Jiang, X.; Yang, X. D.; Wang, L. J.; Wang, Z. H.; Li, L. Q.; Hu, W. P.; Shuai, Z. G.; Li, L.; Zhu, D. *Adv. Funct. Mater.* **2009**, *19*, 272–276.

10.1021/cm900369s CCC: $40.75
Published on Web 04/16/2009

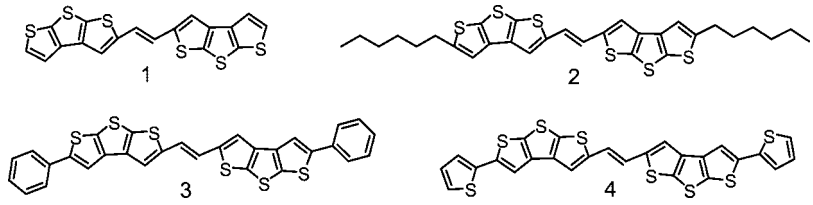

Figure 1. Chemical structure of compounds **1**, **2**, **3**, and **4**.

Scheme 1. Synthetic Routes to Compounds 2, 3, and 4

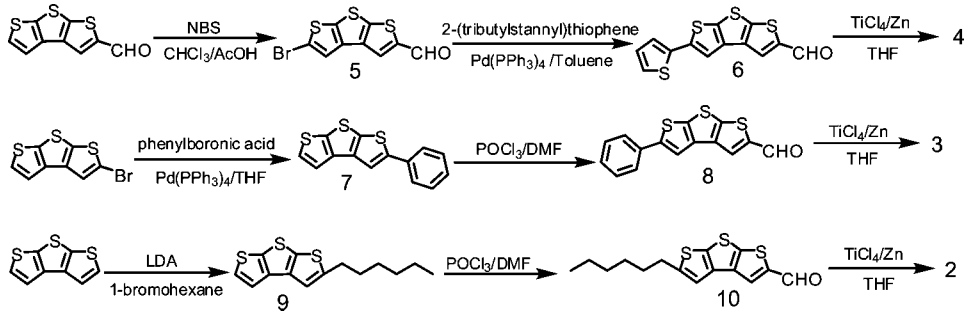

Table 1. Thermal, Optical, and Electrochemical Properties of Compounds 1, 2, 3, and 4

compound	T_{deg}[a] [°C]	T_{DSC}[b] [°C]	λ_{max} [nm] solution[c]	λ_{max} [nm] thin film[d]	E_{HOMO}[e] [V]	E_g[f] [eV]	E_g[g] [eV]
1	342	338	379, 398	339, 423	5.39	2.91	2.48
2	324	236	380, 400	333, 423	5.36	2.94	2.53
3	365	360	381, 400	311, 428	5.41	2.90	2.47
4	336	330	382, 401	359, 404, 431	5.42	2.89	2.34

[a] Degradation temperature (T_{deg}) determined by TGA corresponding to 5% weight loss at 10 °C·min^{-1} under nitrogen flow. [b] Melt point determined by DSC with a scan of 10 °C·min^{-1}. [c] Measurement performed in THF solution. [d] 50 nm thick film deposited by vacuum on quartz. [e] E_{HOMO} determined by cyclic voltammetry (CV) in THF solution. [f] E_g estimated according to the onset of UV absorption in THF solution. [g] E_g estimated according to the onset of UV absorption in thin films.

packing motif to optimize carrier mobility and maintain environmental stability, it is crucial to investigate the effect of the different end substitutions on organic transistor performance. In this contribution, a *trans*-1,2-(dithieno[2,3-*b*:3′,2′-*d*]thiophene)ethene **1** system such as compound **2**, which has two alkyl chains to adjust molecular self-assembly and compounds **3** and **4** which have two phenyl units and thiophene substitutes at both ends to extend conjugation length and/or provide a tight packing, were prepared successfully (Figure 1). In particular, the semiconductors based on compound **3** afford high-performance, air-stable OFET devices with an average mobility as high as 2.0 cm^2 V^{-1} s^{-1} and on/off ratio $\sim 10^8$.

Results and Discussion

Synthesis. The routes to synthesis of compounds **2**, **3**, and **4** are described in Scheme 1. We design three different approaches to synthesize monoaldehyde key intermediates **6**, **8**, and **10**. The last step is McMurry reaction to convert different monoaldehyde functionalities into C=C double bonds, respectively. Lithiation of dithieno[2,3-*b*:3′,2′-*d*]thiophene with LDA to form its anion and subsequent treatment with 1-bromohexane gave the alkylated derivative **9** and a Suzuki coupling reaction of 5-bromodithieno[2,3-*b*:3′,2′-*d*]thiophene, and phenylboronic acid gave phenyl derivative **7**, both of which were readily converted into the corresponding monoaldehydes **10** and **8** via Vilsmier reaction. For synthesis of vinylene-bridged dimer **4**, the intermediate **6** is very important. A Suzuki coupling reaction of 5-bromo-5′-formyl-dithieno[2,3-*b*:3′,2′-*d*]thiophene **5** with 2-thenylboronic acid or phenylboronic acid was initially attempt to achieve monoaldehyde **6** or **8**, but the reactions did not take place. However, the desired compound **6** was finally obtained by Stille coupling of **5** and 2-(tri-*n*-butylstannyl)thiophene in moderate yield. This is likely due to the deboronation of thiophene derivatives in the Suzuki coupling reaction and facilitation of the oxidative addition step in the Stille coupling reaction because of electron-withdrawing groups.[8] The final products were purified by sublimation and characterized by mass spectroscopy (MS), elemental analysis (see Supporting Information), thermogravimetric analysis (TGA), and differential scanning calorimetry (DSC).

Optical and Electrochemical Properties. The UV−vis absorptions of the compounds in THF solution and as thin films are summarized in Table 1. Interestingly, in contrast to the introduction of any aryl groups in both ends of the conjugation system extending a conjugation length,[9] compounds **2**, **3**, and **4** show similar behavior and comparable absorption maxima in solution, which indicate that the substituents do not alter the conjugation length compared

(8) (a) McCulloch, I.; Bailey, C.; Giles, M.; Heeney, M.; Love, I.; Shkunov, M.; Sparrowe, D.; Tierney, S. *Chem. Mater.* **2005**, *17*, 1381–1385. (b) Bao, Z.; Chan, W. K.; Yu, L. *J. Am. Chem. Soc.* **1995**, *117*, 12426–12435.

(9) Boudreault, P. L. T.; Wakim, B.; Blouin, N.; Simard, M.; Tessier, C.; Tao, Y.; Leclerc, M. *J. Am. Chem. Soc.* **2007**, *129*, 9125–9136.

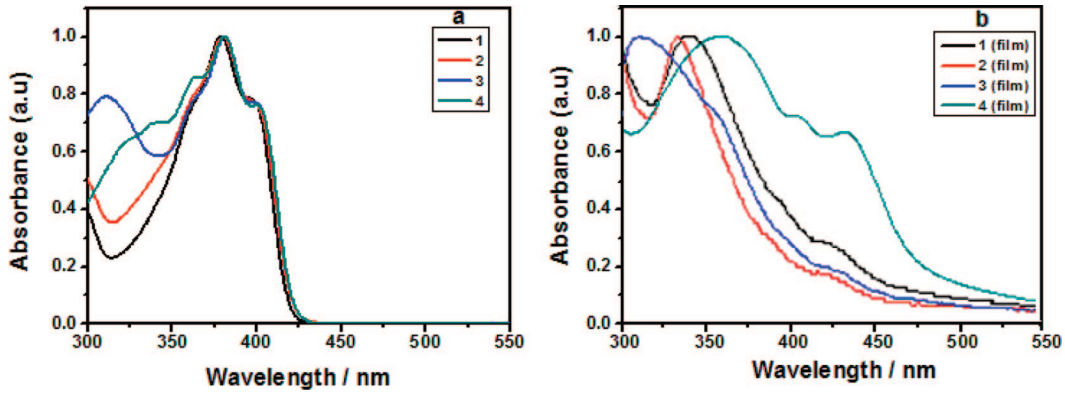

Figure 2. Optical absorption spectra of dimers **1**−**4** in THF solution (a); vacuum-deposited thin films (b).

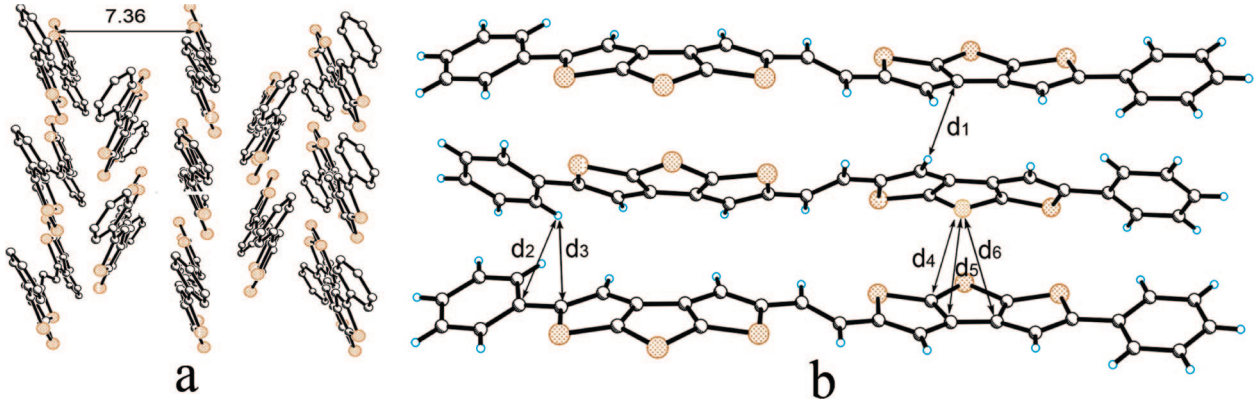

Figure 3. (a) View down the crystallographic *a*-axis of compound **3**; (b) intermolecular interactions in compound **3**; d_1(C···H) = 2.86 Å, d_2(C···H) = 2.88 Å, d_3(C···H) = 2.76 Å, d_4(C···S) = 3.47 Å, d_5(C···S) = 3.35 Å, and d_6(C···S) = 3.41 Å.

with unsubstituted *trans*-1,2-(dithieno[2,3-*b*:3′,2′-*d*]thiophene)ethene. This may be explained in that the central cross-conjugated double bonds in the molecules effectively limit π-electron delocalization between dithieno[2,3-*b*:3′,2′-*d*]thiophene units and phenyl/thiophene groups.[10] However, the dramatic differences are observed in the solid-state absorption spectra (Figure 2). For compounds **1**, **2**, and **3**, the spectra in the solid state are blue shifted relative to solution (H, aggregation). In addition, compound **3** displays a larger blue shift, which suggests compound **3** allows the stronger dipolar interactions among the molecules, while the absorption spectra of compound **4** becomes broadened with a blue shift by 23 nm and a red shift by 30 nm relative to solution. This indicates that there are different types of interactions in the thin film (H aggregation and J aggregation).[11]

The electrochemical properties of these compounds were investigated by cyclic voltammetry (CV) studies, which were performed under nitrogen in 0.1 M THF/TBAPF$_6$ solutions with a scan rate of 100 mV/s. The highest occupied molecular orbital (HOMO) energy levels, estimated from the oxidation onset, vary from 5.30 to 5.50 eV, and the HOMO−LUMO gaps obtained from the absorption onsets vary from 2.89 to 2.93 eV. Judging from these data, we expect that all the compounds are stable semiconductors. It is worth noting that the HOMO levels of all the materials match well with the work function of gold metal (5.2 eV). As a result, the hole injection from the gold source electrode in *p*-type thin-film transistors is expected to be efficient.[12]

Crystallographic Analyses. The single-crystals of compound **3** and **4** are obtained from chlorobenzene solution by slowly cooling from approximately 200 to 80 °C. The single crystal of compound **3** packs in herringbone geometry, similar to compound **1** and pentacene. However, the phenyl ring has a significant effect on the intermolecular interactions. The lateral phenyl groups are twisted by 16.2° in relation to dithienothiophene backbones. As shown in Figure 3b, each phenyl unit has several short phenyl−phenyl contacts and phenyl−dithienothiophenes contacts with two molecules in the adjacent stack. The shortest edge to face interaction distance between the molecules in two adjacent stacks is 3.35 Å, which is slightly shorter than the one measured for compound **1** (3.38 Å) and no S···S interactions are observed. This is at least partially due to the contacts provided by phenyl groups. As expected, the close contacts provide a more dense packing arrangement along the *b*-axis (7.36 Å for **3**, 7.62 Å for **1**, and 7.79 Å for pentacene;[13] see

(10) (a) Rajca, A.; Wang, H.; Pink, M.; Rajca, S. *Angew. Chem., Int. Ed* **2000**, *39*, 4481–4483. (b) Rajca, A.; Miyasaka, M.; Pink, M.; Wang, H.; Rajca, S. *J. Am. Chem. Soc.* **2004**, *126*, 15211–15222. (c) Miyasaka, M.; Rajca, A.; Pink, M.; Rajca., S. *Chem.—Eur. J.* **2004**, *10*, 6531–6539. (d) Miyasaka, M.; Rajca, A.; Pink, M.; Rajca, S. *J. Am. Chem. Soc.* **2005**, *127*, 13806–13807. (e) Miyasaka, M.; Rajca, A. *J. Org. Chem.* **2006**, *71*, 3264–3266.

(11) (a) Zhang, X.; Johnson, J. P.; Kampf, J. W.; Matzger, A. J. *Chem. Mater.* **2006**, *18*, 3470–3476. (b) Zhao, T.; Wei, Z.; Song, Y.; Xu, W.; Hu, W.; Zhu, D. *J. Mater. Chem.* **2007**, *17*, 4377–4381.

(12) Katz, H. E.; Bao, Z. *J. Phys. Chem. B* **2000**, *104*, 671–678.

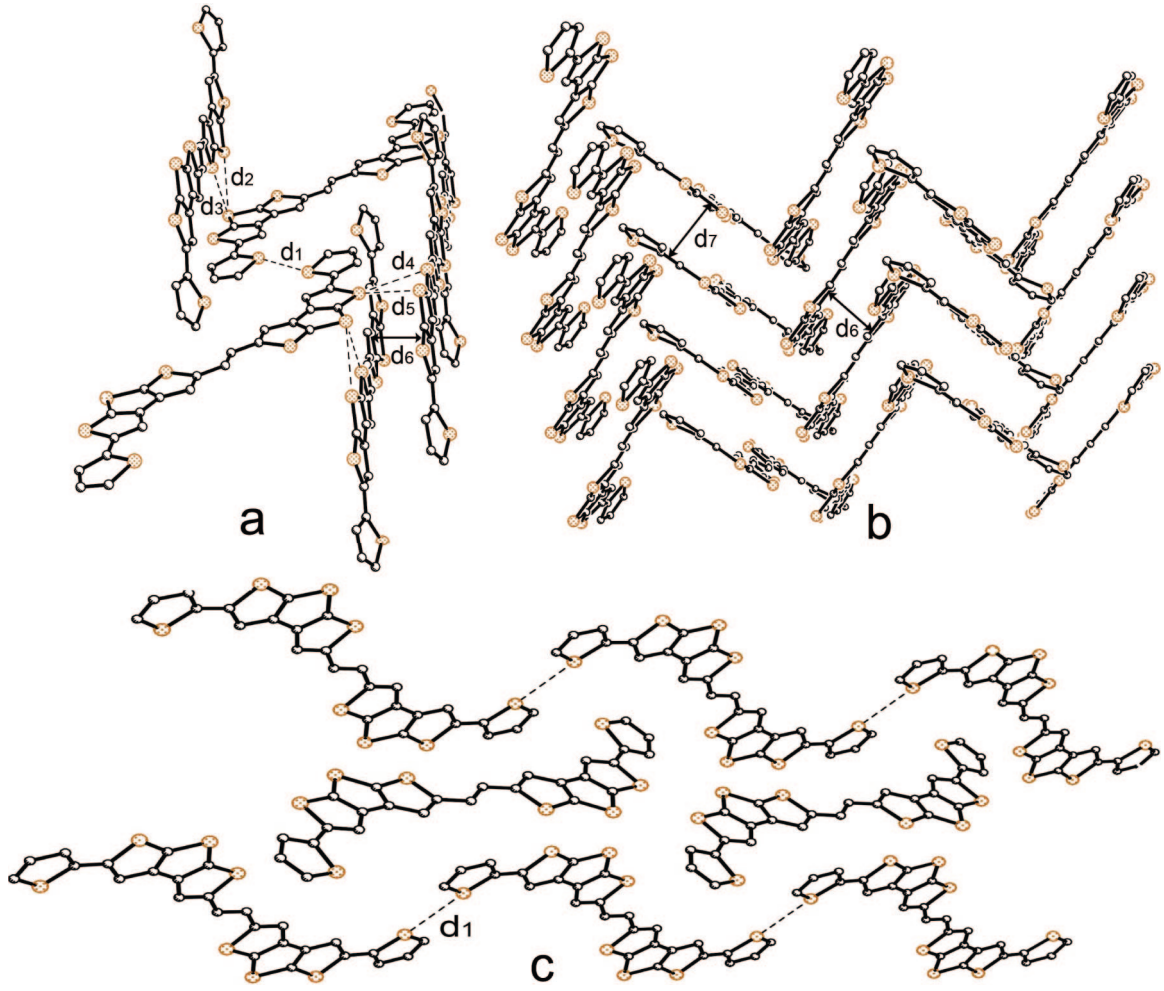

Figure 4. (a) Alternate view of the interstack contacts of compound **4**; d_1(S···S) = 3.40 Å, d_2(S···S) = 3.58 Å, d_3(S···S) = 3.36 Å, d_4(S···S) = 3.58 Å, d_5(S···S) = 3.58 Å, and $d_6(\pi\cdots\pi)$ = 3.48 Å; (b) view down the crystallographic *c*-axis of compound **4**; $d_7(\pi\cdots\pi)$ = 3.34 Å; and (c) view down the crystallographic *a*-axis. Hydrogen atoms were omitted for clarity.

Supporting Information) and produce high carrier mobility in OFETs.

However, compound **4** packs in a strikingly different manner compared to compound **3**. As shown in Figure 4, the substituted thiophene rings change greatly both the molecular arrangement of the dithieno[2,3-*b*:3′,2′-*d*]thiophene cores and intermolecular interactions. It crystallizes in the *P*1 space group and has two inequivalent molecules per unit cell, which have slightly different planar conformations. In contrast to curved compound **3**, the two dithieno[2,3-*b*:3′,2′-*d*]thiophene units are nearly coplanar with respect to each other. The thiophene planes are twisted slightly out of planarity, in relation to dithienothiophene backbones, by approximate 4°. As compared with compound **3**, the molecules are characteristic of slipped face to face π stacking in two different directions. The shortest intermolecular distance between two molecular planes is 3.34 Å, well within the van der Waals radius of the carbon atoms (3.4 Å). The S···S interactions between dithieno[2,3-*b*:3′,2′-*d*]thiophene units bind the molecules in adjacent stacks to cant relative to each other. Interestingly, a distance of 3.40 Å is observed between the sulfur atoms of substituted thiophene rings in different stacks. In this case, both dithieno[2,3-*b*:3′,2′-*d*]thiophene cores and substituted thiophene units provide a three-dimensional electronic coupling in the solid.

Film Microstructure and Morphology. To investigate the crystalline properties of the ring-fused dimers, X-ray diffraction (XRD) patterns were performed on 60 nm films deposited at different temperatures on octadecyltrichlorosilane (OTS) treated substrates. The compound **3** film reveals sharp Bragg reflections up to sixth order diffraction which are assignable to (*h*00) reflections, and it is clear that well-oriented crystalline film is formed. The *d*-spacing (26.6 Å) calculated from the first peak is almost identical to the length of the *a*-axis observed in the single crystal structure (26.3 Å), which indicates the molecule is nearly perpendicular to the substrate with the *bc* plane parallel to the substrate surface. This orientation is well-known to achieve high carrier mobility due to the intermolecular interactions parallel to the direction of the channel current flow.[14] For compound **2**, the reflections up to fifth order are observed, suggesting the formation of high crystallinity on the substrate. However, the *d*-spacing (15.6 Å) is rather small, which may be attributed to the significantly declining orientations of the

(13) Meng, H.; Sun, F.; Goldfinger, M. B.; Gao, F.; Londono, D. J.; Marshall, W. J.; Blackman, G. S.; Dobbs, K. D.; Keys, D. E. *J. Am. Chem. Soc.* **2006**, *128*, 9304.

(14) (a) Gao, J.; Li, R.; Li, L.; Meng, Q.; Jiang, H.; Li, H.; Hu, W. *Adv. Mater.* **2007**, *19*, 3008–3011. (b) Du, C.; Guo, Y.; Liu, Y.; Qiu, W.; Zhang, H.; Gao, X.; Liu, Y.; Qi, T.; Lu, K.; Yu, G. *Chem. Mater.* **2008**, *20*, 4188–4190.

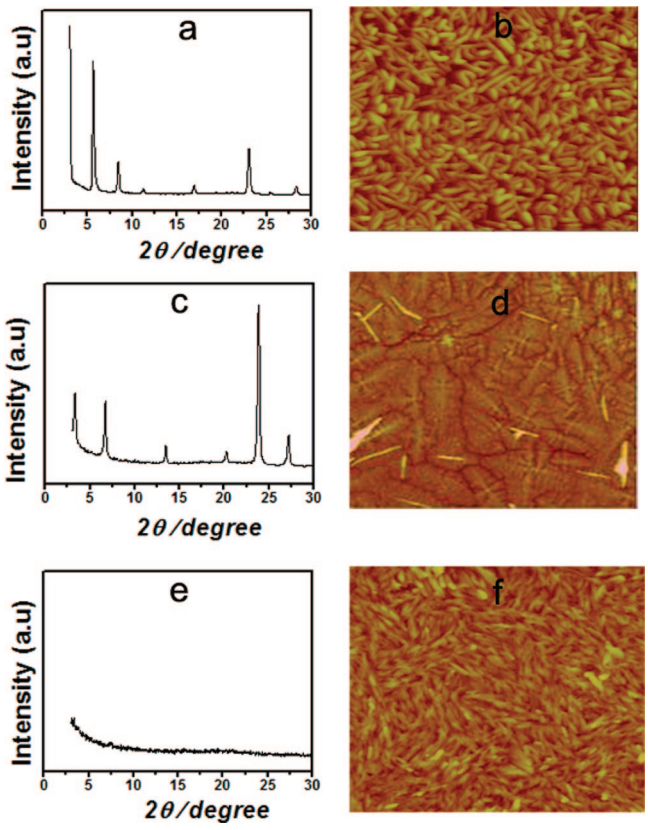

Figure 5. XRD patterns of 60-nm-thick thin films vacuum deposited on OTS-treated Si/SiO_2 at different temperatures: (a, b) compound **2** (100/27 °C); (c, d) compound **3** (100/27 °C); and (e, f) compound **4** (100/27 °C).

molecules on the substrate and cause less favorable intermolecular overlap between dithienothiophenes than compound **3**. On the other hand, no peak is observed in the XRD pattern of **4**, indicating that the films are amorphous and the molecules are randomly oriented in the thin films.

The morphologies of vacuum-deposited thin films under different substrate temperatures were also investigated by atomic force microscopy (AFM). As shown in Figure 5d, the compound **3** forms the thin film in two growth directions (2-D layer), a critical prerequisite to realizing high TFT performances.[4a,b] However, alkyl and thienyl derivatives exhibit one-dimensional growth rather than the other on the substrate due to the prominent packing interactions in one direction, leading to rodlike crystallites in the films (Figure 5b,f), which results in a very high boundary density.[15]

Thin-Film Transistor Device Fabrication and Characterization. Thin film OFETs are fabricated in a "top contact" geometry as reported previously.[7] All the devices are measured in ambient conditions and display p-type properties in air. Figure 6 represents the drain/source (I_{DS}) current and square root of I_{DS} versus gate voltage (V_G) characteristics for the FET devices of compound **3**. Hole mobility calculated in the saturated regime, the threshold voltages, and the on/off ratios obtained at different temperatures are summarized in Table 2. The compound **3** exhibits excellent device performances, with a mobility as high as 0.28 $cm^2\ V^{-1}\ s^{-1}$, and on/off ratio up to 10^6 at room temperature. The mobility slightly increases with the increase of substrate temperatures, and the mobility is 0.84 $cm^2\ V^{-1}\ s^{-1}$ at $T_{sub} = 100$ °C. It is attractive that the compound **3** shows the better mobility of ~2.0 $cm^2\ V^{-1}\ s^{-1}$ and on/off ratio of $\sim 10^8$ by the two-stage deposition process (100/27 °C). Similar to most molecules, which have herringbone arrangement, compound **3** exhibits two-dimensional growth on the surface.[7,15,16] First, 20 nm is evaporated on the substrate under high substrate temperature (100 °C) to form large-size grains on the substrate, and then the cracks and voids between grains are further filled with a second 40 nm deposition at lower (27 °C) substrate temperature. Therefore, the film consists of larger crystalline grains with good connectivity by the two-stage process. This may help account for the increase in mobility for the two-stage process. In sharp contrast, the thienyl-substituted derivative **4** based devices show poor FET characteristics with mobilities on the order of 10^{-3} $cm^2\ V^{-1}\ s^{-1}$, which is almost 3 orders of magnitude lower than that of **3**. This result can be attributed to the amorphous films and the random orientations of the molecules in the thin films. For compound **2**, the introduction of hexyl substituents lowers the device performances relative to their parent molecules, with the highest mobility only at 0.035 $cm^2\ V^{-1}\ s^{-1}$ and on/off ratio 5.8×10^5. It is believed that the higher device performances can be obtained with introduction of side chains due to the self-assembly properties of the alkyl chains.[16b,17] However, here our results suggest the performance of compound **3** is much better than others. This can be explained by their intermolecular interaction differences. According to the UV absorption spectra, the phenyl unit has a great effect on the intermolecular interactions and allows the molecule **3** stronger intermolecular interactions, which are needed to result in smaller packing distances. On the basis of the single-crystal and the XRD analysis, along the crystal packing direction (*b*-axis), which is consistent with the direction of current flow, the crystal packing of compound **3** is more compact. As a result, the charge transport in compound **3** is more efficient.

To test the device stability, we prepare the device based on compound **3** by a two-stage deposition process (100/27 °C) and store it in air. The test is performed under ambient temperature periodically for more than 7 months. As shown in Figure 7, during this period, the fluctuations in the mobilities and on/off ratios are 1.5−2.0 $cm^2\ V^{-1}\ s^{-1}$ and 10^6-10^8, respectively. There is no dramatic change in device performances under long-term operation and storage. The high stability of the devices can be attributed to the large band gap and low HOMO level of the molecule. Thus, this molecule is a promising semiconductor for practical OFET applications.

(15) Valiyev, F.; Hu, W. S.; Chen, H. Y.; Kuo, M. Y.; Chao, I.; Tao, Y. T. *Chem. Mater.* **2007**, *19*, 3018–3026.

(16) (a) Yamamoto, T.; Takimiya, K. *J. Am. Chem. Soc.* **2007**, *129*, 2224–2225. (b) Meng, H.; Sun, F.; Goldfinger, M. B.; Jaycox, G. D.; Li, Z.; Marshall, W. J.; Blackman, G. S. *J. Am. Chem. Soc.* **2005**, *127*, 2406–2407.

(17) (a) Garnier, F.; Yassar, A.; Hajlaoui, R.; Horowitz, G.; Deloffre, F.; Servet, B.; Ries, S.; Alnot, P. *J. Am. Chem. Soc.* **1993**, *115*, 8716–8721. (b) Videlot, C.; Ackermann, J.; Blanchard, P.; Raimundo, J.-M.; Frère, P.; Allain, M.; de Bettignies, R.; Levillain, E.; Roncali, J. *Adv. Mater.* **2003**, *15*, 306–310.

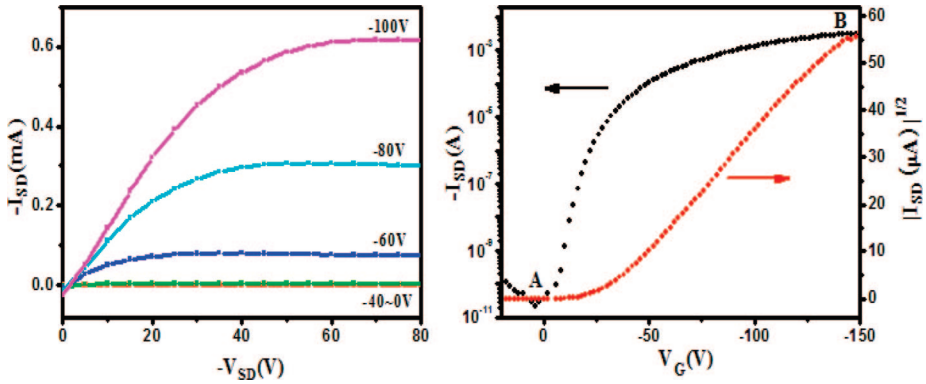

Figure 6. Plots of source-drain current versus source-drain voltage characteristics of the thin film OFETs of **3** deposited at 100/27 °C (left); the transfer characteristics of the devices (right).

Table 2. FET Characteristics of Fuse-Ring Dimers Prepared by Vacuum Deposition on OTS Treated Substrates at Different Temperatures[a]

compound	T [°C]	mobility [cm^2 V^{-1} s^{-1}]	on/off ratio	V_t (V)
2	27	0.035	10^5	−7.0
	100/27	0.038	10^4	−12.0
3	27	0.28	10^7	−28.8
	60	0.54	10^6	−11.5
	100	0.84	10^7	−24.6
	100/27	2.0	10^8	−31.0
4	27	0.0017	10^5	−11.5
	100/27	0.0020	10^4	−13.8

[a] Average mobilities and on/off ratios of 10 devices.

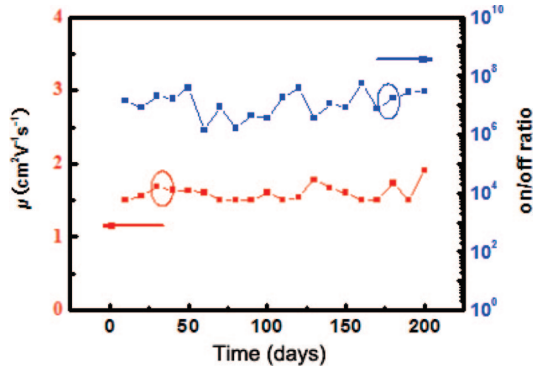

Figure 7. Device performances of compound **3** test over a period of seven months (red, mobility; blue, on/off ratio).

Conclusion

In this contribution, we have prepared three semiconductor materials by chemical modification of compound **1**. A comparative analysis of the optical absorptions, thermal properties, electrochemical potentials, and film morphologies of this system has shown that the molecular packing motifs and interactions have a major effect on the device performances. It has been also observed that the thin-film morphology is very sensitive to the molecular structure, and the 2-D layered film exhibits a high carrier mobility. Although the incorporation of aromatic, alkyl substituents in both ends of **1** have negligible effect on the conjugation length, due to the cross-conjugated double bonds in dithieno[2,3-*b*:3′,2′-*d*]thiophenes building units, the chemical modification leads to great variations in film microstructures, electronic properties, and packing motifs. The appropriate substituents are capable of providing efficient molecular packing arrangements for carrier mobility. For example, the phenyl-substituted derivative **3** demonstrates a remarkably high FET performance, with a mobility up to 2.0 cm^2 V^{-1} s^{-1} and on/off ratio up to 10^8, under optimized device fabrication conditions. Additionally, the devices show good environment stability, even after storage in air for several months.

Experimental Section

Materials Synthesis. The synthesis of *trans*-1,2-(dithieno[2,3-*b*:3′,2′-*d*]thiophene)ethene **5**, 5-bromodithieno[2,3-*b*:3′,2′-*d*]thiophene, and dithieno[2,3-*b*:3′,2′-*d*]thiophene-5-carbaldehyde have already been reported in the literature.[7]

5-Bromo-5′-formyldithieno[2,3-*b*:3′,2′-*d*]thiophene 5. To a solution of dithieno[2,3-*b*:3′,2′-*d*]thiophene-5-carbaldehyde (2 g, 8.9 mmol) in chloroform/AcOH (1:1) was added NBS (1.75 g, 9.8 mmol) at room temperature. The mixture was stirred under argon for 12 h at room temperature and then quenched with water, and the aqueous layer was extracted with chloroform several times. The combined organic phase was washed with saturated brine, dried over magnesium sulfate, and purified by chromatography (1:1 petroleum ether/dichloromethane) to give white crystals (2.4 g, 90%). Mp 163−165 °C; ^{1}H NMR (400 MHz, $CDCl_3$) δ 9.90 (s, 1H), 7.95 (s, 1H), 7.36 (s, 1H), 7.38 (s, 1H); ^{13}C NMR (600 MHz, $CDCl_3$) δ 181.6, 147.0, 145.5, 137.6, 136.9, 136.3, 126.2, 120.9, 113.2; MS (EI) m/z = 303 (M^+). Anal. Calcd for $C_9H_3BrOS_3$: C, 35.65%; H, 1.00%. Found: C, 35.67%; H, 1.25%.

5-Thienyl-5′-formyldithieno[2,3-*b*:3′,2′-*d*]thiophene 6. A solution of 5-bromo-5′-formyl-dithieno[2,3-*b*:3′,2′-*d*]thiophene (1.5 g, 4.9 mmol), tetrakis(triphenylphosphine)palladium (0.46 g, 0.4 mmol), and 2-(tri*n*-butylstannyl)thiophene (2.7 g, 7.34 mmol) in toluene (150 mL) was refluxed at 125 °C for 12 h under argon. The reaction mixture was cooled to room temperature and purified by a short chromatography (1:1 petroleum/dichloromethane) to give yellow solid (0.75, 50%). Mp 172−174 °C; ^{1}H NMR (400 MHz, $CDCl_3$) δ 9.90 (s, 1H), 7.98 (s, 1H), 7.48 (s, 1H), 7.30 (d, 1H, J = 5.2 Hz), 7.24 (d, 1H, J = 5.2 Hz), 7.08 (d, 1H, J = 4.2 Hz); ^{13}C NMR (600 MHz, $CDCl_3$) δ 182.7, 148.4, 146.3, 140.8, 138.5, 138.3, 136.8, 128.0, 127.5, 125.2, 124.5, 115.1; MS (EI) m/z = 306 (M^+). Anal. Calcd for $C_{13}H_6OS_4$: C, 50.95%; H, 1.97%. Found: C, 50.50%; H, 2.35%.

5-Phenyldithieno[2,3-*b*:3′,2′-*d*]thiophene 7. In a two-necked flask were placed 5-bromo-dithieno[2,3-*b*:3′,2′-*d*]thiophene (1.8 g, 6.5 mmol), phenylboronic acid (1.2 g, 9.8 mmol), tetrakis(triphenylphosphine)palladium (0.6 g, 0.52 mmol), THF (20 mL), and 2 M potassium carbonate (5 mL). The mixture was flushed with argon for several times and then heated to 70 °C for 12 h. The reaction mixture was cooled to room temperature, and the organic phase was separated and washed with brine. The crude product was

purified by chromatography (petroleum ether) to give a white solid (1.3 g, 75%). Mp 127−129 °C; ^{1}H NMR (400 MHz, $CDCl_3$) δ 7.65 (dd, 2H, J = 1.3 Hz), 7.59 (s, 1H), 7.41−7.38 (m, 4H), 7.32 (t, 1H, J = 7.2 Hz); ^{13}C NMR (600 MHz, $CDCl_3$) δ 146.9, 138.9, 138.7, 138.1, 134.7, 129.0, 127.7, 125.8, 118.8, 114.7; MS (EI) m/z = 272 (M^+). Anal. Calcd for $C_{14}H_8S_3$: C, 61.73%; H, 2.96%. Found: C, 62.49%; H, 3.05%.

5-Hexyldithieno[2,3-*b*:3′,2′-*d*]thiophene 9. *n*-BuLi (7.7 mmol) was added dropwise to a solution of diisopropylamine (9.2 mmol) in THF (50 mL) at 0 °C. After stirring for 3 h at 0 °C, dithieno[2,3-*b*:3′,2′-*d*]thiophene (1 g, 5.1 mmol) was added to the solution at −78 °C and stirred for another 3 h at −78 °C. 1-Bromohexane (1.3 g, 7.7 mmol) was added to the suspension, and the reaction mixture was then gradually warmed to room temperature. The solution was quenched with water and extracted with diethyl ether. The combined organic phase was washed with saturated brine, dried over magnesium sulfate, and purified by chromatography (petroleum ether) (0.57 g, 40%). ^{1}H NMR (400 MHz, $CDCl_3$) δ 7.39 (d, 1H, J = 5.2 Hz), 7.31 (d, 1H, J = 5.2 Hz), 7.06 (s, 1H), 2.92 (t, 2H, J = 7.6 Hz), 1.75 (td, 1H, J = 7.6, 6.8 Hz), 1.39−1.30 (m, 6H), 0.90 (t, 3H, J = 1.3 Hz); ^{13}C NMR (600 MHz, $CDCl_3$) δ 148.9, 138.6, 138.3, 137.8, 136.1, 127.5, 118.7, 115.9, 31.7, 31.2, 28.7, 22.6, 14.1; MS (EI) m/z = 280 (M^+). Anal. Calcd for $C_{14}H_{16}S_3$: C, 59.95%; H, 5.75%. Found: C, 59.18%; H, 5.51%.

General Procedure for Vilsmeier Reaction. To a solution of dithieno[2,3-*b*:3′,2′-*d*]thiophene derivatives (4.8 mmol) in DMF (20 mL) was added $POCl_3$ (1.8 g, 12 mmol) at 0 °C. The mixture was stirred at for 2 h at 0 °C for 1 h and then at room temperature for 24 h. The resulting suspension was stirred at 50 °C for 5 h and cooled to room temperature. The mixture was poured into ice water, and saturated sodium acetate was added until a PH of approximately 5 was reached; the mixture was stirred for another 3 h. The solution was extracted with dichloromethane, washed with saturated brine, dried over magnesium sulfate, and purified by chromatography using petroleum/dichloromethane (1:1) as eluent.

5-Phenyl-5′-formyldithieno[2,3-*b*:3′,2′-*d*]thiophene 8. Pale yellow crystal (1.3 g, 87%). Mp 165−166 °C; ^{1}H NMR (400 MHz, $CDCl_3$) δ 9.90 (s, 1H), 8.00 (s, 1H), 7.65 (dd, 2H, J = 1.3 Hz), 7.59 (s, 1H), 7.43 (dd, 2H, J = 1.3 Hz), 7.34 (t, 1H, J = 7.2 Hz); ^{13}C NMR (600 MHz, $CDCl_3$) δ 182.8, 149.0, 146.3, 140.1, 138.4, 128.9, 127.7, 118.9; MS (EI) m/z = 300 (M^+). Anal. Calcd for $C_{15}H_8OS_3$: C, 59.97%; H, 2.68%. Found: C, 59.87%; H, 2.86%.

5-Hexyl-5′-formyldithieno[2,3-*b*:3′,2′-*d*]thiophene 10. Pale oil (0.96, 65%). ^{1}H NMR (400 MHz, $CDCl_3$) δ 9.90 (s, 1H), 7.92 (s, 1H), 7.09 (s, 1H), 2.92 (t, 2H, J = 7.6 Hz), 1.75 (td, 2H, J = 7.6, 6.8 Hz), 1.39−1.30 (m, 6H), 0.90 (t, 3H, J = 1.3 Hz); ^{13}C NMR (600 MHz, $CDCl_3$) δ 182.4, 148.2, 138.1, 137.6, 137.2, 136.0, 127.2, 117.7, 115.0, 31.7, 31.2, 28.7, 22.6, 14.1; MS (EI) m/z = 308 (M^+). Anal. Calcd for $C_{15}H_{16}OS_3$: C, 58.40%; H, 5.23%. Found: C, 58.82%; H, 5.43%.

General Procedure for McMurry Reaction. To a suspension of zinc power (2.6 g, 41mmol) in THF (60 mL), titanium tetrachloride (2.2 mL) was slowly added, and the resulting mixture was refluxed for 3 h. A solution of aldehyde (4.1 mmol) and pyridine (3.5 g) in THF (30 mL) was slowly added to the mixture, and the mixture was refluxed for 12 h. After cooling to room temperature, the mixture was diluted with saturated sodium hydrogen carbonate (500 mL) and stirred for 3 h. The solid was filtered and washed with diluted HCl, water, and acetone and dried.

***trans*-1,2-Bis(5-phenyl-dithieno[2,3-*b*:3′,2′-*d*]thiophene)ethene 3.** Yellow powder recrystallized from chlorobenzene (78%). Mp 360 °C; MS (MALDI-TOF) 567.8. Anal. Calcd for $C_{30}H_{16}S_6$: C, 63.34%; H, 2.84%. Found: C, 62.78%; H, 2.92%.

***trans*-1,2-Bis(5-thienyl-dithieno[2,3-*b*:3′,2′-*d*]thiophene)ethene 4.** Orange powder recrystallized from toluene (55%). Mp 330 °C; MS (MALDI-TOF) 580.0. Anal. Calcd for $C_{26}H_{12}S_8$: C, 53.76%; H, 2.08%. Found: C, 54.21%; H, 2.32%.

***trans*-1,2-Bis(5-hexyl-dithieno[2,3-*b*:3′,2′-*d*]thiophene)ethene 2.** Orange powder recrystallized from toluene (80%). Mp 236 °C; MS (MALDI-TOF) 584.2. Anal. Calcd for $C_{18}H_{32}S_6$: C, 61.60%; H, 5.51%. Found: C, 60.86%; H, 5.43%.

Device Fabrication. FET devices were fabricated in the top contact geometry configuration. Thin films were deposited under vacuum on octadecyltrichlorosilane (OTS) modified silicon oxide layers. Gold electrodes were deposited using shadow masks, and the device has a channel length and width of 110 nm and 5.3 μm, respectively. Organic semiconductors were deposited at an initial rate of 0.1 Å s^{-1} then increased to 0.4−0.6 Å s^{-1} gradually under a pressure of about 4.0 × 10^{-6} Torr to a final thickness of 60 nm determined by a quartz crystal monitor. FET characteristics were obtained at room temperature in air on a Keithley 4200 SCS and Micromanipulator 6150 probe station. The mobility of the devices based on the fused-ring oligomers were calculated in the saturation regime. The equation is listed as follows:

$$I_{DS} = (W/2L)C_i\mu(V_{GS} - V_T)^2$$

where W/L is the channel width/length, C_i is the insulator capacitance per unit area, and V_{GS} and V_T are the gate voltage and threshold voltage, respectively.

Acknowledgment. The authors are grateful for financial supports from NSFC (20772131, 20721061, 50725311), 973 Program (2006CB932100, 2006CB806200), and Chinese Academy of Sciences.

Supporting Information Available: CV spectra of compounds **2**−**4** and DSC and TGA measurements of all the compounds (PDF); crystallographic data of compounds **3** and **4** (CIF). This material is available free of charge via the Internet at http://pubs.acs.org.

CM900369S